EUROGRAPHICS Workshop on Graphics and Cultural Heritage (2017)
T. Schreck and T. Weyrich (Editors)

Accurate Soil and Mudbrick BRDF Models for Archaeological Illumination Rendering with Application to Small Finds

V. Badler[1,3], J. Kider Jr.[2], M. Moore[2], B. Walter[4], & N. Badler[3]

[1]Royal Ontario Museum; [2]University of Central Florida; [3]University of Pennsylvania;[4]Cornell University

Abstract

The prevalence of mudbrick structures in the ancient world presents an unexplored opportunity for the realistic portrayal of their appearance. 3D computer models are often constructed from architectural remains to study form and function essential to understanding ancient cultures. These 3D models are usually rendered with estimated colors or photographic images for texture and color reference. Unfortunately, the reflectance properties of soil and mudbrick materials are not well captured in single view photographs. We obtained soil and mudbrick samples from a 1973 excavation of Godin Tepe in Iran and performed a Bi-Directional Reflectance Function (BRDF) capture and analysis on the mudbrick, and both wet and dry soil samples. The resulting BRDFs are used to render the soil and mudbrick interior architecture of the Godin Tepe site. We did illumination studies based on direct sunlight, skydome, and annualized sky irradiance. In a case study we test the archaeological hypothesis that small finds may be found in poorly illuminated portions of enclosed rooms. The accurate sky dome, BRDF surface appearance, and global illumination models are used to assess the applicability and validity of this concept.

1. Introduction

The interaction of light and architecture is of natural interest to archaeologists. Prior to the modern era of electrical light on demand, ancient people were limited to natural light from the sun and moon, and flames from hearths, oil lamps, candles, or torches. The primal importance of celestial events for predictive, empowerment, cultural, or religious needs has a well-established literature in achaeoastronomy (e.g., [Sin05]).

At a personal level, lighting plays a crucial role in illuminating the spaces where people live, work, or worship. Natural light from the sun is exploited for functional or intrinsic beauty (e.g., [GD10]). Large enclosed spaces with roofs for protection from the elements limited sunlight entrances to windows. Often additional internal light sources such as candles, hearths, or oil-filled vessels were used to supplement natural light or provide usability outside daylight hours [HMD*09]. Computational relighting simulations can aid the study of ancient space usage, e.g., [PHKA15] and assessment of visual task feasibility, e.g., [DLGW07]. Sufficient physical light sources could be very effective in illuminating even large enclosed spaces (e.g., [KFY*09]).

The overall archaeological purpose of this study is to determine whether natural lighting influences the locations of excavated small finds, i.e., objects other than pottery. Our hypothesis is that small finds will tend to occur in more poorly illuminated portions of enclosed rooms. Accordingly, we must create visually accurate lighting and appearance models for the excavated structures on a site.

We had access to materials from the ancient Near East Godin Tepe Period VI:1 site, c. 3200-3050 B.C.E. located in central western Iran (Figure 1). During this period, Godin Tepe was a fortified site on the ancient East-West trade route (later called the "Silk Road" ultimately linking the Mediterranean and China) with strong cultural connections to contemporary Late Uruk sites from southern Iraq (Uruk) and southern Iran (Susa). Local Godin Tepe construction methods consisted of mudbrick walls, wooden roofs (charred remains of roof beams were found in room 22 as per plans in Figure 5 of [Bad02]), and presumably lintels for modest structures (Figure 2). These physical constraints led to substantial walls (approximately 0.6 m thick), narrow doorways (again, nominally about 0.5 m to 1 m wide), and limited width, few, or even no windows. These characteristics left meager openings for natural light to enter these enclosed living spaces.

Godin Tepe offers an ideal testbed for our hypothesis that natural lighting influences the locations of excavated small finds. The original site report notes novel circumstances at Godin Tepe which motivate our hypothesis:

> All these data suggest a rapid departure of the inhabitants rather than gradual abandonment and slow decay. On the other hand, there is no stratigraphic or structural evidence of deliberate or violent destruction. This conclusion is supported by the kinds of small finds found. Pottery, broken jar sealings, tablets, tablet fragments and other objects of clay are numerous. Yet metal was rare, and precious metals and stones were missing entirely. In

DOI: 10.2312/gch.20171289

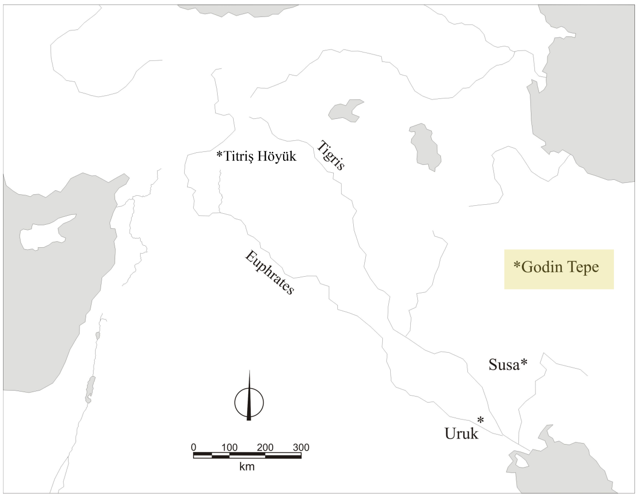

Figure 1: *The Near Eastern region showing the geographical location of the excavated Godin Tepe site c. 3200-3050 B.C.E. and the related modern ethnographic village resource located next to the site of Titriş Höyük.*

Figure 2: *The Godin Tepe Period VI:1 excavation in 1973.*

> short, the valuable items which could and would be carried off in a hasty but planned retreat are missing. Other items of less value, which might have been carried off had the abandonment been more leisurely, were left in situ. Certainly a more complete selection of finds, such as might result from sudden violent destruction, is not present. [WYJ75] (Note: In this publication at this time Godin Tepe Period VI:1 was referred to as Period V.)

Interior space illumination may be reconstructed in 3D using computer graphics. Appropriate placement of light sources and accurate surface material reflectance properties yield realistically lit images [HMD*09]. With considerable artistic care, natural lighting for a Neolithic room at Çatalhöyük has been reconstructed using computer graphics global illumination methods [Cox]. A reflectance model analytically defines the response (reflection) of a surface to incident light. Surfaces may be generally reflective (mirror-like), specular (shiny), or diffuse; the latter scatter light in all directions (like rough surfaces and flat finish paint). Unplastered mudbrick is a diffuse reflector; whitewashed or plastered finishes on mudbrick can make it more specular. Global illumination may therefore play an important role in diffusing light through enclosed spaces otherwise nearly devoid of direct light from the surrounding sky dome.

We organize the discussion by describing our methodology for modeling the Godin Tepe architecture, for illuminating the site, and for computing surface reflectance of actual site mudbrick and soil samples. We give examples of small finds that were located in two rooms within relatively dark areas, and conclude with observations about future studies.

2. 3D MODELS AND ASSUMPTIONS

To test the hypothesis of whether natural lighting influences the locations of small finds, we examined rooms from the excavations at Godin Tepe Period VI:1 (Figure 3). We constructed a 3D representation of the excavated architecture and ground levels based on the published plans [Bad02] using Maya 2017 and Renderman 21 [Ren].

The ground mesh was constructed so that each face was one square meter and lined up exactly with the Godin Tepe 1973 Period VI:1 Deep Sounding Oval Complex image scaling. The ground is slightly sloped, starting higher toward the north at rooms 15 and 17 and ending lower to the south around rooms 4 (the entrance) and 5. The site elevations show some smaller local bumps and height variations, which are transferred onto the modeled ground plane. The height of all the wall niches and floor transition thresholds are taken directly from the Godin Tepe site measurements. Some archaeological assumptions were made about the architecture. (a) The ceilings were 1.85 m high, with (b) a wooden board at the top of every doorway and window that extended 0.3 m down from the ceiling. (c) The height of the western fortification wall was set at 2.2 m and (d) the exterior buttress heights were set to 1 m. (e) Rooms 2a, 22, and 23 (cut off by the limits of the excavation) were assumed to have walls on all sides. (f) We assumed that all rooms had a roof, except the center courtyard (room 1).

3. COMPUTING DIRECT ILLUMINATION

The Godin Tepe Period VI:1 courtyard, room 1, is not roofed, and therefore in full light. Some rooms (3, 10, 14, 19, and 20) are enclosed with one door leading to the courtyard. Room 18 has two windows overlooking the courtyard, and others are interior rooms with a doorway leading into another room (12, 13, 15, 17, and 23).

Because the rooms have thick walls, small doorways, few or no windows, and presumably solid ceilings, very little direct sunlight falls on the interior floors. To establish a direct illumination baseline we integrating the visible sky dome (hemisphere) for every square meter ground area. This technique is related to computing ambient occlusion [Mil94] for rendering, but we are only interested in the sky dome visibility. Ambient occlusion is used for archaeological rendering in [Cox], but only in its usual sense of the local environment, not the distant sky dome.

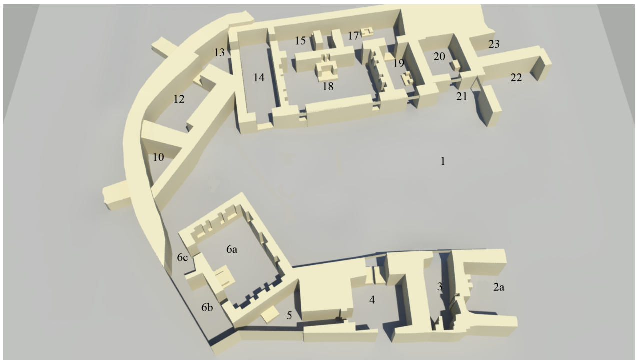

Figure 3: *This image shows the 3D model of Godin Tepe during Period VI:1 (with no ceilings). Rooms are numbered according to the original excavation. The sunlight matches the sun position on September 21, 3200 B.C.E, at 8:00 am. North is vertical in the image. The excavation limits to the east and south cut off rooms 2a, 22, and 23; they are unlikely to be as open as modeled.*

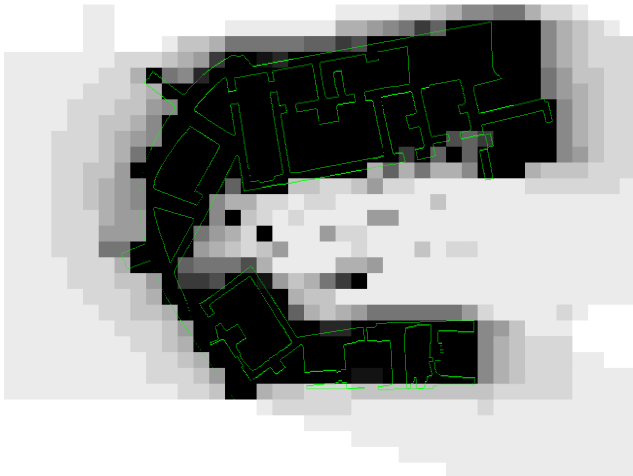

Figure 5: *Godin Tepe during Period VI:1 with the percentage of sky hemisphere exposure scaled from 0 (black) to full sunlight (white).*

Figure 4: *The sun position was calculated using the altitude and azimuth for Sept 21, 3200 B.C.E, at 2:00 pm. A ray was cast from the center of each ground square to the sun. If no objects (walls or roof) intersected the ray, the square was in sunlight and is shown in white; otherwise, the square was in shade and is shown in black.*

ROOM	FLOOR	ARRAY DIMS	AREA
Whole Site	40x30	$1200m^2$	$1.00m^2$
Room 1	30x30	$100m^2$	$0.111m^2$
Room 18	40x30	$33.3m^2$	$0.0278m^2$
Room 20	30x30	$11.1m^2$	$0.0123m^2$

Table 1: *Site and room sample square sizes. This shows the dimensions of the arrays and their actual areas used to accumulate the light exposures. Each square is a face in the direct illumination computation.*

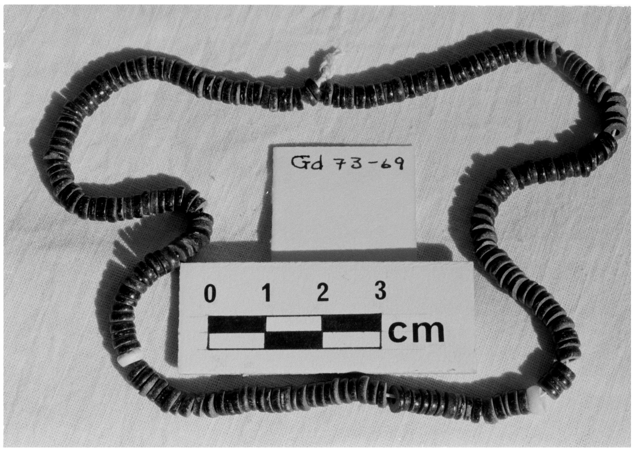

Figure 6: *The Godin Tepe Period VI:1 beaded necklace, C. 3200-3050 B.C.E. Courtesy of the Royal Ontario Museum,* ©ROM.

Various small finds were excavated in Godin Tepe Period VI:1, e.g., a beaded necklace (Figure 6). We speculated whether these were lost or abandoned in places where they would not be seen under daylight illumination conditions. To test this hypothesis we investigated three sunlight models. The first was direct sun illumination, the second used the complete sky dome, and the third added indirect illumination to interior spaces.

For direct sun illumination we used the NASA HORIZON Web-Interface to calculate the altitude and azimuth of the sun for the times and dates of interest and at solstice and equinox. We found, however, that very little floor area within the rooms actually received direct (full) sunlight (Figure 4). We then modified our approach to consider what fraction of the entire sky dome (hemisphere) illuminated each square meter area on the floor (Figure 5). To simulate the sky we looked at the accuracy of various sky models ([KKN*14]) to get the most realistic illumination from the sky dome. The pseudo-code for this is given as Algorithm 1. This approach appears to be the more robust of the two approaches and is less dependent on season, time of day, and sun position. (For sun and sky radiation maps with global illumination see Figure 17 for room 18 and Figure 15 for room 20.)

Algorithm 1: Pseudo-code for Malley's method to compute uniformly distributed points on a hemisphere.

```
for i ← 0) to 200 do
    samplePoint = Calculate uniformly random point on unit
      hemisphere using Malley's Method
end
for j ← 0) to numFaces do
    center = Calculate center of face rayIntersection(center,
      samplePoint)
    if (rayIntersection == false) then Sunlight[j]++
end
maxSun = 0
for j ← 0) to numFaces do
    if (Sunlight[j] > maxSun) then maxSun = Sunlight[j]
end
for j ← 0) to numFaces do
    faceColor = Sunlight[j] / maxSun //squareColor =
      faceColor * white //Set all pixels in square to be
      squareColor
end
```

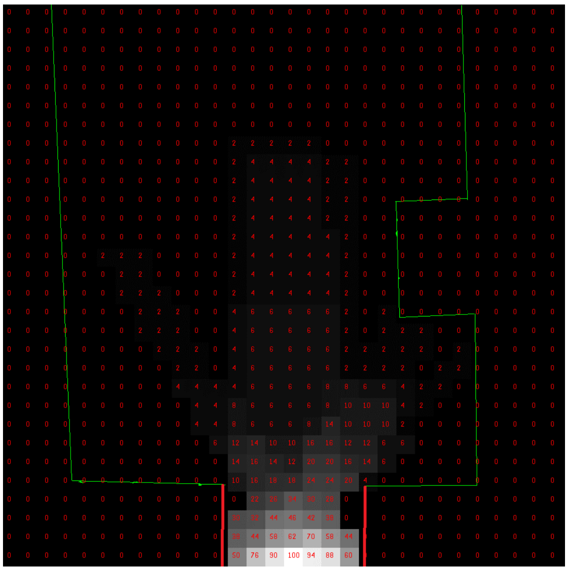

Figure 7: *Illuminated areas of room 20. The numbers are the* relative *percentage of unoccluded rays out of 200 probes per square to the sky hemisphere. The southernmost center square has 50 rays out of 200, thus it was the most illuminated (100%). A hearth occupies the center of the eastern wall.*

Malley's method is used to compute uniformly distributed points on a hemisphere [PH10]. The result of this computation is a heatmap of exposures where each floor cell counts the number of unblocked rays from that square that hit the sky hemisphere. Figure 7 shows the relative illumination result for room 20; the maximum exposure (relative 100%) is the center of the doorway (50 out of 200 sky samples). Only a few squares even come close to seeing 10% of the sky area. Figure 8 shows the sky dome direct illumination map for room 18, using absolute sample counts per square out of the 200 probes.

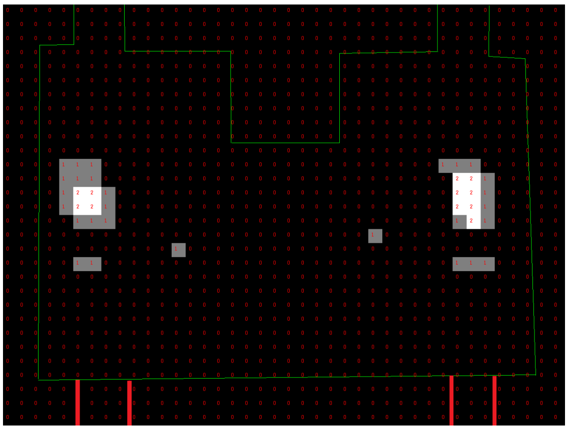

Figure 8: *Room 18 sky exposure. The numbers are the count of unoccluded rays out of 200 probes per square to the sky hemisphere. The windows are outlined in red at the southern exposure. A hearth occupies the center of the northern wall. Two flanking doorways lead to other windowless rooms to the north.*

4. Capturing Realistic BRDFs

While direct illumination is a significant factor in lighting ancient sites, the materials used for construction, such as mudbrick, are mostly diffuse and must play some role in spreading light though more of the interior. To accurately and realistically render the model and its indirect illumination, we captured the Bidirectional Reflectance Distribution Function (BRDF) of dirt and mudbrick samples from the actual Godin Tepe site (loaned from the Royal Ontario Museum). We used a spherical *Gantry* to obtain BRDFs directly from the samples. This gantry is a room-sized goniometer, consisting of two computer-controlled arms, one with a light source and the other with a DSLR camera, that sweep concentric shells around an object platform (Figure 9). We used a Macbeth chart for color correction, and small markers for alignment between the different camera captures. The light source for the gantry was a white point light source that rotated to different angles. The light source can be seen on the right side of Figure 9.

The BRDF is a four dimensional function that describes how light is reflected at an opaque surface. The BRDF provides the reflectance of a target as a function of the viewing geometry and the illumination. We had access to two different mudbrick samples from the Godin Tepe architecture, and dirt samples from two different rooms. We measured BRDFs in three conditions: dry, then wet, then dried. To capture this data requires the gantry to fix a light source location, and rotate the DSLR receiver to different locations. For a relatively complete sample of the BRDF we moved the point light source 60 times, repeatedly capturing the receiver images. Some sample data is given in Figure 12 which visualizes a few Low-Dynamic Range (LDR) images with varying light angles.

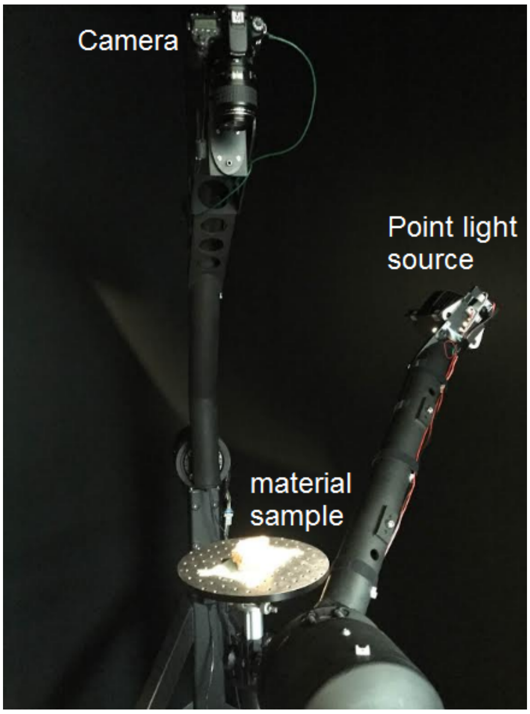

Figure 9: *The spherical Gantry at Cornell used to capture the Godin Tepe mudbrick and dirt sample BRDFs. The camera (top), and point light source (right) rotate around the sample (bottom).*

This Figure shows how the samples look under different lighting angles. For the final BRDF fitting we used 60 light angles per camera position and captured High-Dynamic Range (HDR) image sets (4-6 photos each) at each stop. LDR images are not sufficient to capture the reflectance behavior of the small remnants of plaster and dirt, thus HDR techniques are necessary.

Figure 10: *Mudbrick wall samples from Godin Tepe, excavated lot Gd 73 A2 1189. The larger sample on the right has remnants of plastering, a common practice for mudbrick surfaces.*

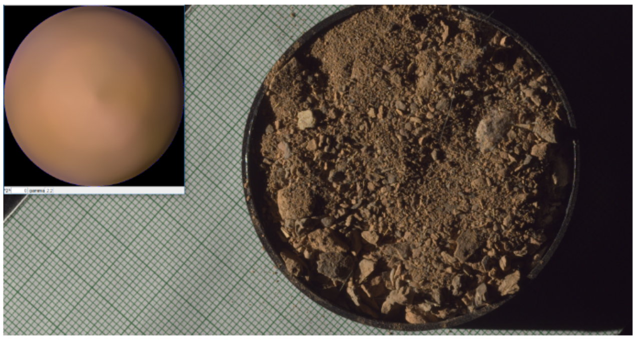

Figure 11: *Dirt sample from the Godin Tepe site and a corresponding BRDF slice*

established with the Gantry.

Once we capture this HDR dataset, we can use the markers to align all the images, then select and average a small group of pixels across all the images (some of which are shown in Figure 12). Now we have discrete points in the 4D BRDF space (Figure 11). We interpolate the missing points based on the nearest neighbors and construct the full BRDF. A few sample slices of the BRDFs of all the samples we captured are shown in Figure 13. This demonstrates how the BRDFs are close to, but not perfectly, diffuse (based on the light angle). These samples also differ visibly in the dry or wet, and plastered or unplastered states.

This process created a unique dataset of real material reflection properties as BRDFs from the Godin Tepe samples. This method is extensible to other sites and is more accurate and robust than previous analog photographic methods for capturing color appearance which are highly dependent on numerous unknowns such as sunlight conditions, film speed, film type, exposure time, developing variables, etc. Using this data we developed two BRDF plug-ins (in Renderman). The first plug-in is run directly from the BRDF data samples, and fills in the missing angles by looking at the 9 nearest neighboor samples and running a weighted average. The second plug-in fits the data to the OrenâĂŞNayar reflectance model giving a simple lambertian model based on the average color and reflectance. Our rendered results primarily use the data-driven plug-in.

5. Results

There were several small finds in Rooms 18 and 20 from Godin Tepe Period VI:1. Both of these rooms had hearths, and the excavation records show that both hearths had significant evidence of burning. These hearths were contemporaneous with the small finds.

A significant small find in this occupation level was a necklace of 208 black beads and two white beads with a total length of about 21 cm (Figure 6). The beads were found in a cluster in the southeast corner of room 20; the organic material used to string the necklace had decayed. (The excavation Daily Log for June 14, 1973 states explicitly: “Against W-AJ, in corner with W-AG”, i.e., literally in the southeast room corner.) From Figure 7 it can be seen that no squares in this area receive any direct light from the sky hemisphere at all.

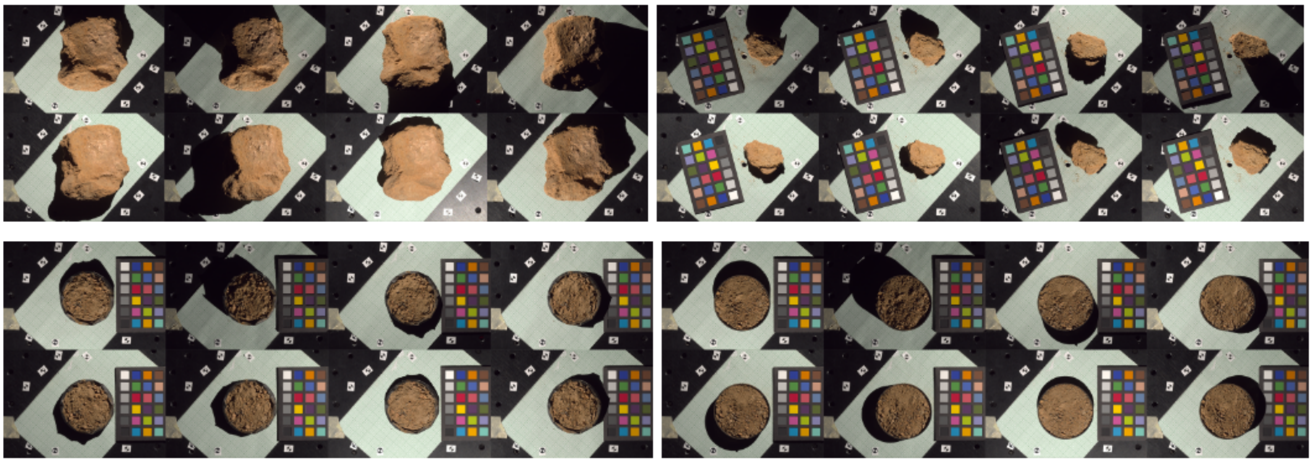

Figure 12: *This figure shows a few sample capture angles for the two mudbrick samples and the two dirt samples from the Godin Tepe site. We used a Macbeth chart for color correction and markers to help rectify and align all the images.*

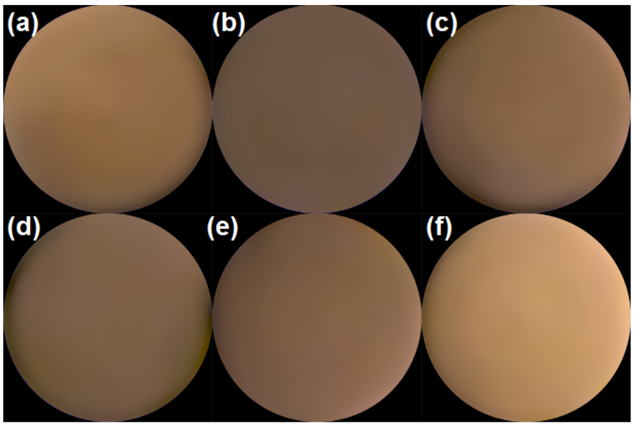

Figure 13: *This shows a slice of the BRDF results for (a) the large mudbrick sample, including visible evidence of a plastered surface, (b) dirt sample 479, (c) dirt sample 517, (d) dirt sample 479 (wet then dried), (e) dirt sample 517 (wet then dried), (f) the small (unplastered) mudbrick sample.*

Since we can now compute accurate reflection models, we placed a typical fire in the hearth, used an emission spectrum appropriate to wood fuel, and rendered the room with Renderman. The view facing the bead necklace corner find spot (circled) is shown in Figure 14. From the image it is apparent that even with the addition of the global illumination from the proper wall material, the corner is still in relative darkness. Standard reading light levels fall between $300-500$ lux and this circled region representing the corner findspot is computed to be only 9 lux. To be visible in the Figure at all, the image is tone mapped: we use the Reinhard et al. technique [RSSF02] followed by gamma correction to tonemap recorded HDR radiance values to the low dynamic printable range. The beads' black color would have also contributed to their being inconspicuous. The hearth fire does not directly illuminate that corner. Moreover, the relative bright light from the sky dome visible through the doorway actually would make it more difficult to see in the corner, due to the eye's accommodation to bright illumination.

To avoid lighting condition specificity, we then used Radiance [War94] to calculate *annual* irradiation at floor node locations. This provides an annualized daylight irradiance heat map. This simulation utilized both direct lighting from the sun, indirect lighting from the skydome, and realistic weather data from data collected in Iran. We set the Radiance ambient bounce to 8 to account for the indirect global illumination from the sun and sky. Figure 15 visualizes the irradiance on the floor of room 20. Note that the absolute illumination in the southeast corner findspot (circled) is very small.

Other small finds came from room 18; a Renderman rendering is shown in Figure 16. One metal pin, one metal needle, and one stone bead with grooves were found near the hearth at the north side. One metal bird-shaped object, one metal pin point, five stone beads, and one incised stone bead were found next to the inside south wall in between the two windows. These findspots (circled) are in areas of darkness even considering global illumination from the natural materials and hearth fire. Again, with standard reading light levels between $300-500$ lux, these findspots have very dim computed values of 4 and 22 lux. Looking at Figure 8, the direct sun illumination is weak but concentrated in the middle in line with the two thick windows (red lines) in the south wall facing the courtyard. An additional architectural observation can be made from this illumination pattern. Room 18 apparently functioned as a distribution center, as it contained almost 2,000 unbaked clay slingballs [Bad05]. The south-facing windows would facilitate this function for the workers inside. The annualized natural light distribution shown in the room 18 floor plan rendered by Radiance (Figure 17) has a maximum concentration toward the rear and is very well aligned with the placement of those north side door thresholds. Thus the room 18 windows would have provided some indirect light to the windowless back rooms (15 and 17) to the north due to the strategic placement of the two internal doorways.

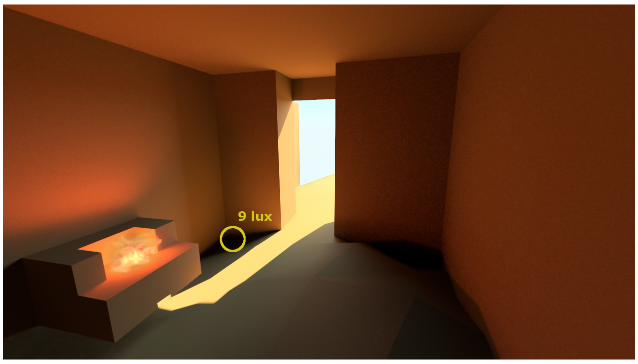

Figure 14: *Room 20 rendered with measured BRDFs for the mudbrick and dirt, and computed lux value at the findspot. With realistic sky illumination and a hearth fire, the room is accurately rendered but remains dark at the bead necklace find spot (yellow circle).*

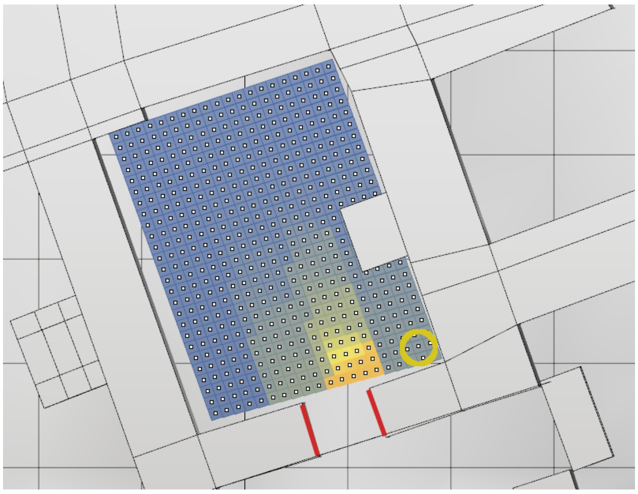

Figure 15: *Room 20 rendered as a daylight illumination heatmap. This visualizes the annual irradiation at floor node locations. The yellow circle denotes the findspot for the bead necklace.*

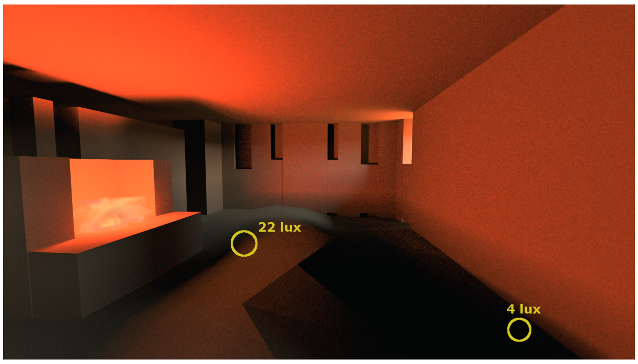

Figure 16: *Room 18 rendered with measured BRDFs for the mudbrick and dirt, and computed lux values at the findspots. With realistic sky illumination and a hearth fire, the room is accurately rendered but remains dark where the small finds were located (yellow circles): [left circle] one pin, one metal needle, and one stone bead with grooves were found near the hearth at the north side; [right circle] one metal bird-shaped object, one metal pin point, five stone beads, and one incised stone bead were found next to the inside south wall in between the two windows.*

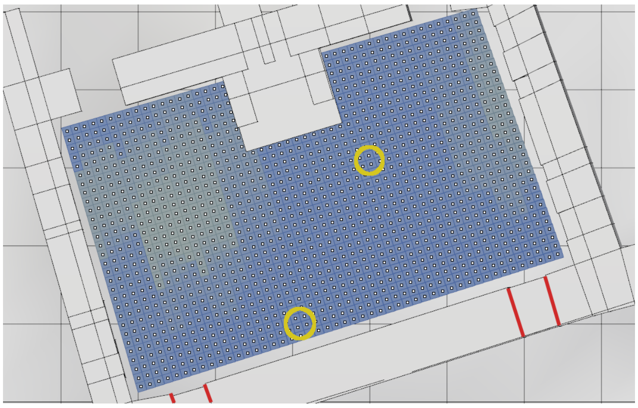

Figure 17: *Room 18 heat map showing relative daylight illumination on the floor. This visualizes the annual irradiation at floor node locations. The yellow circles denote the known findspots: [upper right circle] one metal pin, one metal needle, and one stone bead with grooves were found near the hearth at the north side; [lower left circle] one metal bird-shaped object, one metal pin point, five stone beads, and one incised stone bead were found next to the inside south wall in between the two windows.*

6. CONCLUSIONS

Although mudbrick has been subjected to diffuse reflectance analysis, primarily for differentiation and provenience studies [BDA07], we have not seen measured reflectance distribution functions suitable for computer graphics rendering. Additional factors that influence reflectance, such as texture and grain size, are notably variable even on the same site [Lov12]. The presence of smooth plastering will also influence reflectivity by increasing specularity. The investigation of sunlit areas in ancient sites will be essential to any realistic recreation of their interior appearance.

We have used actual excavation site samples of dirt and mudbrick from Godin Tepe in Iran to measure accurate material BRDFs. These were applied to the surfaces of a 3D architectural model and the terrain substrate yielding visual appearance that is much better than adapting colors derived from photographic plates. Moreover, the BRDFs allow global illumination algorithms to create realistic interior renderings. This technique is adaptable to any site where soil and construction material samples and a suitable BRDF measurement system is available. Such samples are portable, in contrast to “in situ” studies such as the Parthenon stone BRDFs [CDPS06] measured by Debevec et al. [TSE*04]. Given extant samples held in museums, this method can be applied to reconstruct global illumination in ancient, perhaps now inaccessible, sites, especially those built from soil and mudbrick materials. In addition, wet and dry BRDFs permit new ways of looking at ancient site appearance.

Accurate BRDFs yield a good visualization of interior illumination within architectural spaces. Figures 16 and 14 demonstrate the feasibility of creating global illumination renderings of natural and fire-lit interior spaces. Actual ceiling reflectivity characteristics at Godin tepe are unknown. Any known openings through the ceiling to access the roof would provide additional skylight paths to the interior [Cox], and can be readily rendered. However, based on informal ethnographical fieldwork at another Near Eastern site, Titriş Höyük, Turkey, ceiling openings are not found in the living rooms but rather in storage spaces. Figure 18 shows the relative darkness of a modern mudbrick living space.

Figure 18: *Relative darkness of a modern mudbrick living space with a hearth fire but no ceiling openings. Shot in mid-afternoon during summer 1995 with natural light on 1000 ASA 35 mm film.*

Measured BRDFs of local building materials and soil create the visual appearance of naturally illuminated spaces in ancient life. Much interior space is dark. We verified that the most valuable small find for this occupation period, the beaded "necklace," was indeed found in a corner that was extremely dark under sunlit conditions, even with a hearth fire.

7. Acknowledgments

We are grateful to the Royal Ontario Museum, Toronto, Canada and its staff for allowing us to analyze the mud brick fragments, especially Dr. Clemens Reichel, Associate Curator, World Cultures and Bill Pratt, Collection Technician, Egypt and West Asia. Without their kind cooperation, this analysis could not have been accomplished. We also acknowledge the late Dr. Cuyler Young, Jr., who in 1973 excavated the Period VI Deep Sounding of Godin Tepe. Dr. Guillermo Algaze of the University of California, San Diego, kindly allowed Virginia Badler to participate in the excavations at Titriş Höyük, Turkey.

References

[Bad02] BADLER V. R.: A chronology of Uruk artifacts from Godin Tepe in central western Iran and implications for the interrelationships between the local and foreign cultures. *Artefacts of Complexity: Tracking the Uruk in the Near East 5* (2002), 79–109. 1, 2

[Bad05] BADLER V. R.: *The Buildings of Godin Tepe Period VI:1B, Deconstruction and Virtual Reconstruction*. The Canadian Society for Mesopotamian Studies, Bulletin 40, 2005, pp. 57–64. 6

[BDA07] BALSAM W., DEATON B., ADLER M.: Analysis of adobe wall composition at the Chaves-Hummingbird site, New Mexico, by diffuse reflectance spectrophotometry. *Geoarchaeology 22*, 8 (2007), 825–844. 7

[CDPS06] CALLIERI M., DEBEVEC P., PAIR J., SCOPIGNO R.: A real-time immersive application with realistic lighting: The Parthenon. *Computers & Graphics* (2006), 368–376. 7

[Cox] COX G.: Archaeological computing systems: An investigation into the potential of the Mental Ray engine to artificially represent light in the Neolithic site of Çatalhöyük. URL: https://grantcoxmedia.files.wordpress.com/2011/04/archaeological-computing-systems-final.pdf. 2, 8

[DLGW07] DAWSON P., LEVY R., GARDNER D., WALLS M.: Simulating the behaviour of light inside arctic dwellings: Implications for assessing the role of vision in task performance. *World Archaeology 39*, 1 (2007), 17–35. 1

[GD10] GRUBER E., DOBBINGS J.: Illuminating historical architecture: The house of the drinking contest at antioch. *Fusion of Cultures, Abstracts of the XXXVIII Conf. on Computer Applications & Quantitative Methods in Archaeology* (2010), 421–424. 1

[HMD*09] HAPPA J., MUDGE M., DEBATTISTA K., ARTUSI A., GONÃĞALVES A., CHALMERS A.: Illuminating the past. *Int. Symp. on Virtual Reality, Archaeology & Cultural Heritage* (2009). 1, 2

[KFY*09] KIDER J., FLETCHER R., YU N., HOLOD R., CHALMERS A., BADLER N.: Recreating early Islamic glass lamp lighting. *Proc. International Symposium on Virtual Reality, Archaeology, & Cultural Heritage (VAST)* (2009). 1

[KKN*14] KIDER JR. J. T., KNOWLTON D., NEWLIN J., LI Y. K., GREENBERG D. P.: A framework for the experimental comparison of solar and skydome illumination. *ACM Trans. Graph. 33*, 6 (Nov. 2014), 180:1–180:12. 3

[Lov12] LOVE S.: The geoarchaeology of mudbricks in architecture: A methodological study from Çatalhöyük, Turkey. *Geoarchaeology 27*, 2 (2012), 140–150. 7

[Mil94] MILLER G.: Efficient algorithms for local and global accessibility shading. In *Proceedings of the 21st Annual Conference on Computer Graphics and Interactive Techniques* (New York, NY, 1994), SIGGRAPH '94, ACM, pp. 319–326. 2

[PH10] PHARR M., HUMPHREYS G.: *Physically Based Rendering: From Theory To Implementation*, 2nd ed. Morgan Kaufmann, San Francisco, CA, 2010. 4

[PHKA15] PAPADOPOULOS C., HAMILAKIS Y., KYPARISSI-APOSTOLIKA N.: Light in a Neolithic dwelling: Building 1 at Koutroulou Magoula (Greece). 1034–1050. 1

[Ren] Renderman21. URL: https://renderman.pixar.com/view/renderman. 2

[RSSF02] REINHARD E., STARK M., SHIRLEY P., FERWERDA J.: Photographic tone reproduction for digital images. *ACM Trans. Graph. 21*, 3 (July 2002), 267–276. 6

[Sin05] SINCLAIR R. M.: The nature of archaeoastronomy. *Current Studies in Archaeoastronomy: Conversations Across Time and Space* (2005), 3–13. 1

[TSE*04] TCHOU C., STUMPFEL J., EINARSSON P., FAJARDO M., DEBEVEC P.: Unlighting the Parthenon. In *SIGGRAPH 2004 Sketches* (New York, NY, 2004), SIGGRAPH '04, ACM, pp. 80–. 7

[War94] WARD G. J.: The RADIANCE lighting simulation and rendering system. In *Proc. Annual Conference on Computer Graphics & Interactive Techniques* (New York, NY, 1994), SIGGRAPH '94, ACM, pp. 459–472. 6

[WYJ75] WEISS H., YOUNG JR. T. C.: The Merchants of Susa. *Iran 13*, 1 (1975), 1–17. 2